International Dairy Journal 39 (2014) 316–323

Contents lists available at ScienceDirect

International Dairy Journal

journal homepage: www.elsevier.com/locate/idairyj

Enhanced characterisation of milk fat globules by their size, shape and refractive index with scanning flow cytometry

Anastasiya I. Konokhova [a], Andrey A. Rodionov [a, b], Konstantin V. Gilev [a, b], Ilya M. Mikhaelis [a, b], Dmitry I. Strokotov [a], Alexander E. Moskalensky [a, b], Maxim A. Yurkin [a, b], Andrei V. Chernyshev [a, b], Valeri P. Maltsev [a, b, c, *]

[a] Institute of Chemical Kinetics and Combustion, Institutskaya 3, 630090, Novosibirsk, Russia
[b] Novosibirsk State University, Pirogova 2, 630090, Novosibirsk, Russia
[c] Novosibirsk State Medical University, Krasny Prospect 52, 630091, Novosibirsk, Russia

ARTICLE INFO

Article history:
Received 25 April 2014
Received in revised form
4 August 2014
Accepted 5 August 2014
Available online 19 August 2014

ABSTRACT

We present a high-precision method for characterisation of a milk sample by the distributions over milk fat globules (MFG) size, shape, and refractive index (RI). We measured light-scattering profiles of individual MFGs and used global optimisation to retrieve their characteristics. We tested two optical models, a sphere and an oblate spheroid, and found that the latter is a more adequate model for part of the MFGs. We applied the developed method to samples of raw bovine milk and milk from two commercial manufacturers. Diameter and RI of individual MFGs were determined with median errors of 74 nm and 0.0094, respectively, which proves the method to be sensitive to small changes in the MFG properties. Moreover, the distributions over size, surface area, and RI showed a good sensitivity to the details of the milk treatment. In particular, the MFG specific surface area is significantly different for all three milk samples studied.

© 2014 Elsevier Ltd. All rights reserved.

1. Introduction

Since 1674, when Van Leeuwenhoek observed milk fat globules (MFGs) using primitive microscopy, the physical and colloidal properties of these globules have been investigated with different physical methods. This interest has been caused by a role that milk fat plays in health and diseases (Berner, 1993; Spitsberg, 2005). At present, this role is related to different areas of human health, ranging from the obesity problem (Berton et al., 2012) to clearance of apoptotic cells (Lauber et al., 2013). Additionally, the MFGs are responsible for, or contribute to, some of the properties and phenomena observed in liquid dairy products, and are essential to the manufacturing and characteristics of many dairy products (Huppertz & Kelly, 2006).

Surface area can be considered the most important characteristic of the globules, because they are surrounded by a membrane composed of bioactive molecules like proteins, phospholipids, triglycerides and enzymes (Freudenstein et al., 1979; Lopez, 2011; Singh, 2006). Proteins of the globule membrane interact with milk proteins (Su & Everett, 2003) and microflora (Beresford, Fitzsimons, Brennan, & Cogan, 2001), forming natural bioactive nutrition. The globule membrane is sensitive to modification during isolation and processing, and care should be taken to standardise the composition and characteristics of the membrane to maintain its unique properties during application in food products (Dewettinck et al., 2008). Homogenisation, different types of pasteurisation, sterilisation, etc., can substantially change the surface area of the MFGs of milk samples (Fauquant, Briard, Leconte, & Michalski, 2005). Homogenisation exerts the most dramatic effect on the globules changing their size distribution (Ong, Dagastine, Kentish, & Gras, 2010; Thiebaud, Dumay, Picart, Guiraud, & Cheftel, 2003) and surface proteins (Zamora, Ferragut, Guamis, & Trujillo, 2012).

The mechanisms leading to a particular size distribution of MFGs and changes in their mean size are not well-documented and are still under investigations. The question, "What is the role played by the size distribution of MFGs?" (Lopez, 2011) forces us to develop methods for measurement of this distribution with

* Corresponding author. Tel.: +7 383 3333240.
E-mail address: maltsev@kinetics.nsc.ru (V.P. Maltsev).

http://dx.doi.org/10.1016/j.idairyj.2014.08.006
0958-6946/© 2014 Elsevier Ltd. All rights reserved.

modern physical approaches which provide highest precision in determination of a size and surface area of MFGs.

Instrumentally, MFGs were analysed with different physical methods such as ordinary (Van Kreveld, 1942), holographic video (Cheong, Xiao, & Grier, 2009) and confocal (Fucà, Pasta, Impoco, Caccamo, & Licitra, 2013; Gallier, Gragson, JimeNez-Flores, & Everett, 2010; Ong et al., 2010) microscopy, dynamic light scattering (Robin & Paquin, 1991), ultrasound (Miles, Shore, & Langley, 1990), scanning flow cytometry (Maltsev, Chernyshev, Semyanov, & Soini, 1997; Soini, Chernyshev, Hänninen, Soini, & Maltsev, 1998), small-angle light scattering (Michalski, Briard, & Michel, 2001), and electrical impedance (Hillbrick, McMahon, & Deeth, 1998). These methods analyse either individual particles consequently or a large population of particles at once. For example, the small-angle light-scattering method, implemented in a laser diffraction particle size analyser, is currently most widely used to measure the size distribution of MFGs (Garcia, Antona, Robert, Lopez, & Armand, 2014). This method, based on the measurement of light scattering from particle suspensions, has substantial fundamental limitations in inversion of a size distribution from a diffraction pattern without a priori information. Alternatively, an instrument based on single-particle analysis generally leads to better precision of the particle characteristics because it utilises only an optical model of a single particle but assumes nothing about the size distribution. Moreover, all above mentioned methods assume that an MFG can be optically modelled by a homogeneous sphere characterised by a size and refractive index (RI). The current trends in milk studies require the measurement of MFG size distribution with nanometer precision (Argov, Lemay, & German, 2008). Such precision may only be reached with simultaneous determination of size and RI of an individual globule, since otherwise uncertainty in the RI will introduce bias in determined size values. There are only two methods capable of determination of both characteristics of a homogeneous sphere – scanning flow cytometry and holographic video microscopy. The latter was used for high-precision measurement for MFG size and RI (Cheong et al., 2009) albeit at relatively low statistic (sample size up to 100).

Most important applications of the scanning flow cytometry relate to characterisation of morphology of biological cells, in particular, blood cells. It was applied to analysis of spherised red blood cells (Semyanov, Tarasov, Soini, Petrov, & Maltsev, 2000), mononuclear cells (Strokotov et al., 2009), blood platelets (Moskalensky et al., 2013), and rod-like bacteria (Konokhova, Gelash, Yurkin, Chernyshev, & Maltsev, 2013). Aggregates composed by two spheres were successfully characterised by polarised scanning flow cytometer with determination of six characteristics of an aggregate (Strokotov, Moskalensky, Nekrasov, & Maltsev, 2011). At present the scanning flow cytometry allows one to characterise individual non-spherical and inhomogeneous particles with a rate of 300 particles per second (Maltsev, Chernyshev, & Strokotov, 2013). A single spherical particle can be sized with a precision as good as 5 nm (Strokotov et al., 2011). In this study we demonstrate the applicability of the scanning flow cytometry to characterisation of MFGs by their size, surface area, and RI. We obtained the highest precision of individual MFG characteristics among alternative methods, suggesting the scanning flow cytometry as the reference method of MFG characterisation.

2. Materials and methods

2.1. Milk samples

Raw whole bovine milk was obtained from a local individual farmer (Novosibirsk, Russian Federation) and was kept at 4 °C for up to 6 h before analysis. Two other milk samples were obtained from different commercial manufacturers, they are further labelled by their fat content – 2.5% and 3.2%. The manufacturing of both commercial milk samples was done according to the Russian standard GOST R 52090-2003 “Drinking milk and milk beverage. Specifications”, which includes homogenisation, pasteurisation, and standardisation. All samples were warmed to approximately 20 °C prior to measurement and diluted 50,000 times with distilled water. Three milk samples (raw, 2.5%, and 3.2%) were measured with the original scanning flow cytometer (SFC) analysing 6600, 6700, and 7200 individual MFGs respectively.

2.2. Scanning flow cytometer

To determine particle characteristics from light scattering we used the following workflow: light-scattering measurement → particle identification → optical model of the particle → theoretical simulation of light scattering → solution of the inverse light-scattering (ILS) problem. To perform the light-scattering measurements of MFGs, the SFC was used as a commercial prototype fabricated by CytoNova Ltd Company (http://cyto.kinetics.nsc.ru/; Novosibirsk, Russia). Contrary to a conventional flow cytometer that measures forward (FSC) and side (SSC) light-scattering signals, the SFC additionally measures the angle-resolved light-scattering profile (LSP) of an individual particle (Maltsev, 2000). A detailed description of the current set-up of the SFC was given elsewhere (Maltsev et al., 2013). Here, we briefly describe the schematic optical layout of the SFC shown in Fig. 1. The part of the SFC formed by Laser 2 (488 nm, 15 mW, FCD488-020, JDS Uniphase Corporation, Milpitas, CA, USA), Objective 1, flow cell (FC), Objective 2, and side scattering (SSC) detector is identical to an ordinary flow cytometer. The SSC detector generates side-scattering signal to trigger the electronics of the SFC. The other part formed by Laser 1 (405 nm, 30 mW, Radius, Coherent Inc., Santa Clara, CA, USA), Polariser, quarter-wave plate (QWP), FC, and LSP Detector generates the LSP of individual particles carried by a flow. The polariser and QWP provide circular polarised incident radiation for measurement of the LSP used in the solution of the ILS problem.

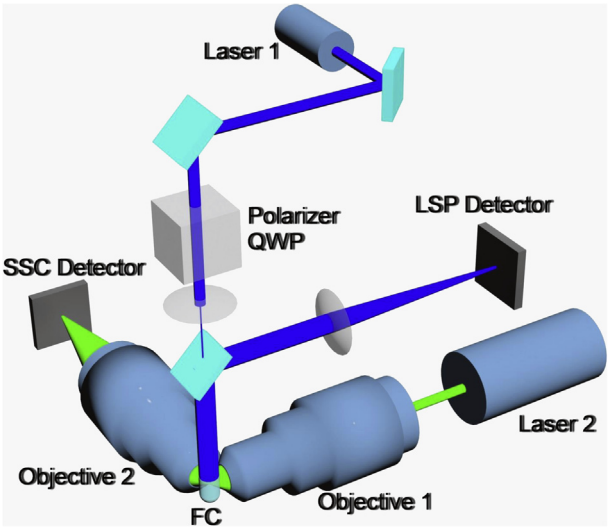

Fig. 1. Schematic layout of the Scanning Flow Cytometer. The following optical elements are shown as abbreviations: FC, flow cell; QWP, quarter-wave plate; SSC Detector, side-scattering detector; LSP Detector, light-scattering profile detector.

2.3. Optical model of milk fat globule

The MFGs can be easy identified from SFC measurements because of a small size of casein micelles (low scattering) and a low concentration of bacteria. Hence, following the above mentioned workflow, we developed an appropriate optical model of an MFG. The optical model of a particle is usually formed based on microscopic studies of the particles. These studies have shown that one can obviously use a sphere as an optical model of an MFG for those methods which are limited by diffraction resolution, 300–400 nm in MFG diameter. The sub-diffraction resolution, i.e., tens of nanometers, requires one to take into account specific details of the particle shape. Actually MFGs have a weak asphericity, which can be precisely ascertained from confocal microscopy with typical resolution of 150 nm. In particular, the analysis of the confocal images of the MFGs showed that the axial ratio of MFGs was varied from 1 to 1.3 especially for large-sized MFG fraction (Garcia et al., 2014; Fig. 1). Electron micrographs lead to similar conclusions (El-Zeini, 2006; Fig. 1b; Zamora et al., 2012; Fig. 5). The nonspherical shape of MFGs can be explained by their complex secretion process (Heid & Keenan, 2005), in contrast to seed-growth mechanism that generally leads to spherical shape.

Based on the above mentioned reasons, we used both a sphere and an oblate spheroid as the optical models for MFGs. From light-scattering point of view, an oblate spheroid is characterised by the following: equi-volume diameter (d_{ev}), axial ratio (ε), and RI (n). The d_{ev} is defined as the diameter of the sphere having the same volume, and we use the term diameter for it in the rest of the paper to facilitate comparison with the spherical model. The orientation of the spheroid relatively to the directions of propagation and polarisation of the incident radiation must be taken into account to simulate light scattering. Generally, this orientation is defined by two Euler angles α and β. However, the measured LSP (Eq. (1) below) is independent of α, leaving β, the angle between direction of propagation and spheroid symmetry axis, as the only relevant one. Thus, the spheroidal model has four variables: d_{ev}, ε, n, and β, while a sphere – only two variables: diameter (d) and RI (n).

2.4. Light-scattering theoretical simulations

The next stage of the workflow relates to theoretical simulation of light scattering from MFGs. The proposed optical model for an MFG, an oblate spheroid, allows us to use the T-matrix method (Mishchenko & Travis, 1998; Mishchenko, Travis, & Mackowski, 2014) to simulate light scattering from these particles. To simulate light scattering from a homogeneous sphere, we used the Mie theory (Bohren & Huffman, 1983; Wriedt, 2008). Taking into account the circular polarisation of the light from Laser 1 (Fig. 1) and axial symmetry for a sphere and oblate spheroid, the theoretical LSP $I_{\mathrm{LSP,th}}$ was simulated with the following formula (Yurkin et al., 2005):

$$I_{LSP,th}(\theta, d_{ev}, \varepsilon, n, \beta) = k \int_0^{2\pi} S_{11}(\theta, \varphi)\mathrm{d}\varphi, \tag{1}$$

where S_{ij} is the Mueller matrix (Bohren & Huffman, 1983), and θ and φ are polar and azimuth scattering angles. The k is the scaling coefficient that relates the scattering signal in mV to the scattering efficiency of a particle calculated from a scattering theory. The value of coefficients k was determined from the calibration of the SFC by 2 μm polystyrene microspheres. We used the wavelength of 405 nm in simulation of the LSPs.

2.5. Inverse light-scattering problem

In this study, we utilised the global optimisation for solution of the ILS problem, which is critical due to complicated dependence of LSP on particle characteristics (Strokotov et al., 2009). The global optimisation requires us to select the regions in which the MFG characteristics are varied. According to the literature we used the following regions: d_{ev} from 0.5 to 6 μm, ε from 1 to 1.4, n from 1.44 to 1.55, β from 0° to 90°. Previously, we used two algorithms of global optimisation: DiRect (Jones, Perttunen, & Stuckman, 1993; Strokotov et al., 2009) and nearest-neighbor interpolation using the pre-calculated database of LSPs (Moskalensky et al., 2013). The first algorithm is an iterative one based on numerous solutions of direct light-scattering problem, which is suitable for spherical model due to fast simulations with the Mie theory. By contrast, the T-matrix method is too time consuming (few seconds per one LSP), hence, is more suitable for database-based algorithm.

The next important component of minimisation algorithm is the appropriate objective function S specifying the difference between experimental and theoretical LSPs. We specified this function as a sum of two terms: the ordinary weighted sum of residual squares (Strokotov et al., 2009) and the squared residual of the peak position, P_{FFT}, in the amplitude Fourier spectrum of the LSP (Semyanov et al., 2004), resulting in

$$S(d_{ev}, \varepsilon, n, \beta) = \sum_{i=1}^{N} \left[w(\theta_i) \cdot \left[I_{LSP,th}(\theta_i, d_{ev}, \varepsilon, n, \beta) - I_{LSP,exp}(\theta_i) \right] \right]^2 + 0.1 \cdot \left[P_{FFT,th}(d_{ev}, \varepsilon, n, \beta) - P_{FFT,exp} \right]^2, \tag{2}$$

where $w(\theta_i)$ is the weighting function

$$w(\theta) = \frac{1^\circ}{\theta} \exp\left(-2 \ln^2(\theta/54^\circ) \right), \tag{3}$$

$I_{LSP,exp}$ is the experimental LSP, and $P_{FFT,th}$ and $P_{FFT,exp}$ are the Fourier peak positions for the theoretical and experimental LSPs respectively. The weighting factor 0.1 in front of the second term in Eq. (2) was determined empirically minimising the mean standard error over the regions of the MFG characteristics.

Both above algorithms not only minimise the function S and determine the best-fit model characteristics or their mathematical expectations, but also estimate their errors (uncertainties or, equivalently, standard deviations of the probability distribution) based on the Bayesian method (Moskalensky et al., 2013). Moreover, the latter adequately responds (by larger errors of characteristics) to model errors, e.g., when a non-spherical particle is fitted by a spherical model (Strokotov et al., 2009). Applying both models to each MFG, we chose the best model on a single-particle basis. For that, we applied the F-test using the null hypothesis of spherical model with 5% significance level. Specifically, the “combined” algorithm chooses the result of spheroidal or spherical models, if the latter can or cannot be reliably rejected, respectively. Similar discrimination can be obtained by comparing errors of MFG diameter of two models or by the width of the confidence region of ε for spheroidal model (data not shown).

3. Results and discussion

3.1. Milk fat globule characterisation from light scattering

First of all, we verified the sensitivity of the LSP to the shape of oblate spheroids. The theoretical LSPs of oblate spheroids with

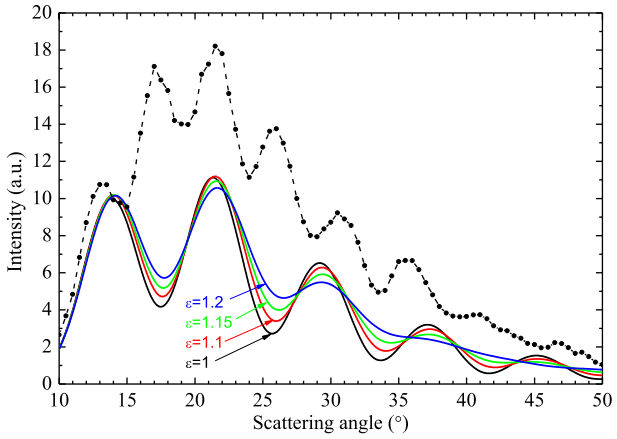

Fig. 2. The theoretical light-scattering profiles of sphere and oblate spheroids (solid lines) and experimental light-scattering profile of milk fat globule (points) measured with the scanning flow cytometer (d_{ev} = 2.2 μm; n = 1.48; β = 80°).

different axial ratios (including sphere) are shown in Fig. 2. The LSPs are hereinafter presented in the weighted form, i.e., Eq. (1) multiplied by weighting function (Eq. (3)). The weighted LSP measured with the SFC for a single MFG (with somewhat different characteristics) is also shown in Fig. 2 for qualitative comparison. The oscillation amplitude of the LSPs falls down with increasing ε, especially in the angular interval from 30 to 50 degrees. The similar behaviour (flat tail) is present in the experimental LSP in Fig. 2, as well as in substantial fraction of all measured LSPs (data not shown), which qualitatively explains the importance of using spheroidal model, at least for some of the MFGs.

We measured 6600 LSPs of MFGs from the sample of raw milk for approximately 1 min. The LSPs were processed by the sphere- and spheroid-based algorithms (Section 2.5), determining the characteristics of the individual MFGs. The results of characterisation of six typical MFGs are shown in Fig. 3. There are three rows in the figure: the first row (A) demonstrates near perfect agreement between experiment and theory, the second row (B) demonstrates the most common agreement and third row (C) demonstrates good agreement. In each row the MFGs from different size regions are shown (larger sizes in the right column). We emphasise that this approach also estimates the errors of characteristics of individual MFGs. The diameter error generally increases with particle size, but significantly varies from particle to particle. Still, even the largest diameter errors of the combined method, shown in bold typeface in Fig. 3(C2), is 190 nm, which is approximately equal to the diffraction limit for this wavelength. For most of the measured MFGs the precision is much better, in particular half of the MFG diameters were measured with an error smaller than 74 nm (see Table 1 for details).

Next we discuss the shape of the MFGs. The inversion algorithm allowed us to separate of MFGs into two fractions: those well-described by a sphere and those requiring a spheroidal model (according to the F-test). The distributions over diameter for these fractions are shown in Fig. 4. We stress, however, that such definition of sphericity is highly method-dependent. In particular, the MFGs that are well-described by a sphere are not necessarily

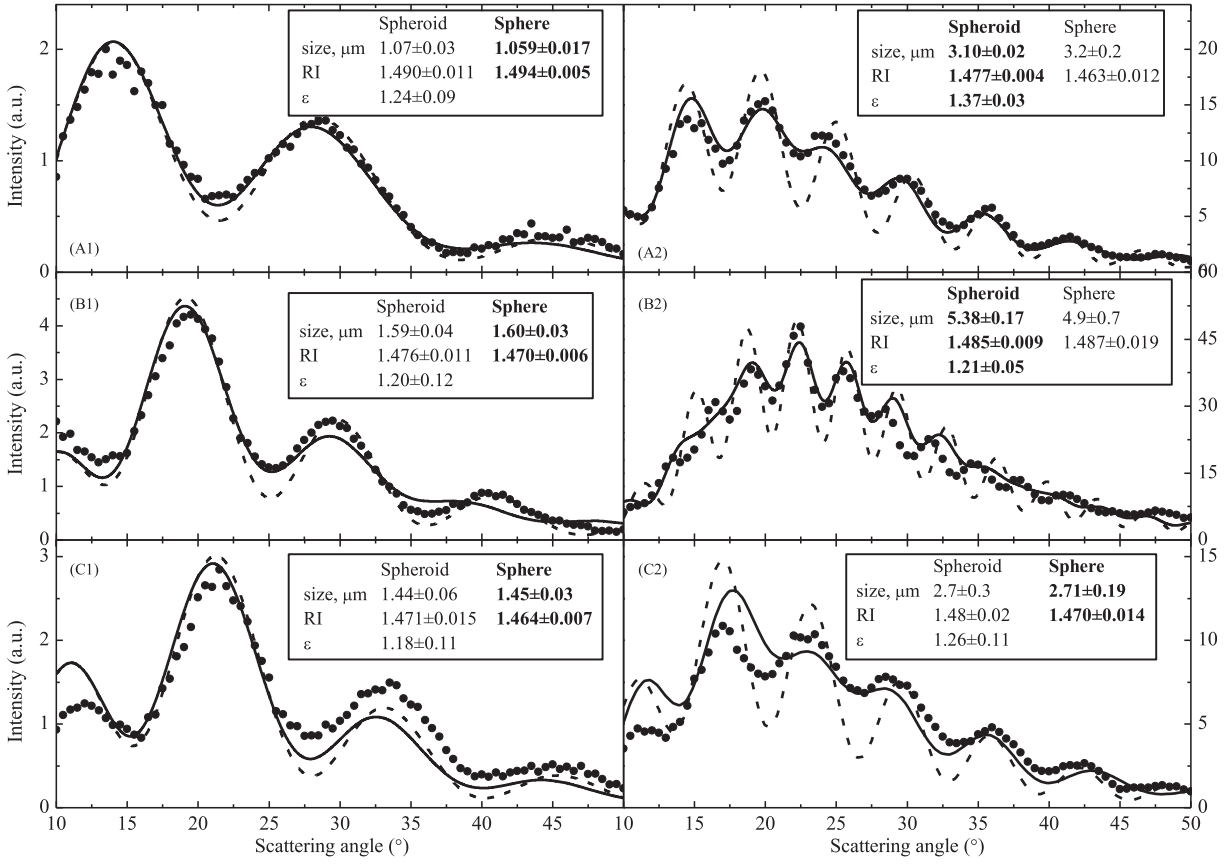

Fig. 3. The result of solution of the inverse light-scattering problem for individual milk fat globules. Experimental light-scattering profiles (●), nearest from spheroid database (solid line), best-fit sphere (dashed line). Insets show the characteristics obtained with different optical models (mathematical expectations ± standard error). Bold typeface indicates the model selected by the combined algorithm.

Table 1
Parameters of milk fat globules distributions of the raw milk sample processed by iteration (sphere), database (spheroid) algorithms, and final results (combined).

Parameter	Sphere	Spheroid	Combined
Diameter (μm)			
Mean ± standard error of mean	2.276 ± 0.012	2.278 ± 0.013	2.285 ± 0.012
Standard deviation	1.004	1.022	1.022
Median	2.174	2.163	2.175
Refractive index			
Mean ± standard error of mean	1.47329 ± 0.00015	1.47808 ± 0.00016	1.47429 ± 0.00017
Standard deviation	0.0120	0.0132	0.0143
Surface area (μm^2)			
Mean ± standard error of mean	19.4 ± 0.2	19.7 ± 0.2	19.8 ± 0.2
Standard deviation	16.0	17.0	16.9
Median	14.9	14.8	14.9
Specific surface area (μm^{-1})	1.95	1.93	1.93
Well-described by spheres (%)	100	0	71
Error of diameter (nm)			
Mean	159	138	119
Standard deviation	167	118.3	122
Median	80	104	74
Error of refractive index			
Mean	0.0114	0.0150	0.0106
Standard deviation	0.0056	0.0041	0.0051
Median	0.0098	0.0153	0.0094

spheres, i.e., have value of ε very close to 1 (if measured, e.g., by electron microscopy). Instead they may have such size that the LSP is insensitive to ε (and β), which is the case for the smallest MFGs (data not shown). Alternatively, when the variation of LSP with ε is comparable to experimental errors, the spheroidal model may even overfit the experimental LSP resulting in larger diameter errors, see, e.g., Fig. 3 (A1). Similar behaviour may be observed for aggregates of MFGs, which are known to be present in microscopic images (Garcia et al., 2014; Fig. 1). Such aggregates are characterised by large model errors, i.e., both sphere and spheroid models are not adequate, and we suspect Fig. 3(C1) and (C2) to be corresponding examples. However, for the smallest monomers the aggregate of two MFGs may be significantly better described by spheroidal model, since the LSP is less sensitive to shape difference smaller than the wavelength, which may explain the small-size peak in spheroidal fraction in Fig. 4.

While the spherical model is sufficient, or even beneficial, for a large part of MFGs, the spheroidal model is still required for another significant part (overall 29%, but a dominant fraction of larger MFGs, Fig. 4), resulting in up to 10 times decrease of diameter errors, see, e.g., Fig. 3A2 and 3B2. Those MFGs are definitely non-spherical, which may affect the results of other sphere-based methods to characterise MFGs, such as low-angle light-scattering or video holography microscopy. However, the results of this paper cannot be applied directly; instead a separate analysis (sensitivity test) should be carried out for a particular characterisation method and size range of MFGs.

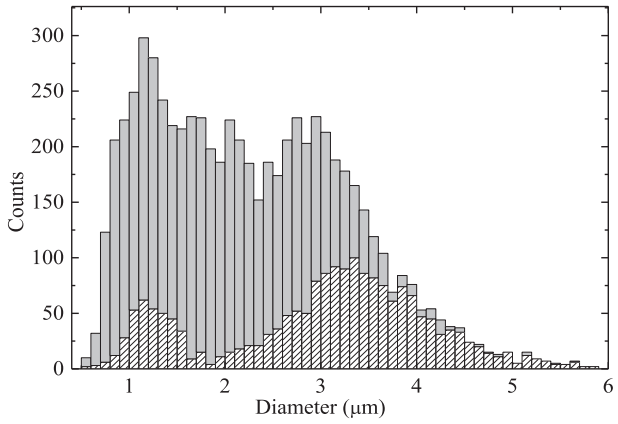

Fig. 4. The distribution (stacked histogram) of milk fat globules in raw milk sample over diameter, separated into those well-described by a sphere (■) and those requiring spheroidal model (▨).

Finally, we tested the mutual consistency of estimated confidence ranges for d and n using different optical models for each MFG using the Z-test, and 99% of measured MFGs passed the test at 95% confidence level. This additionally validates that both methods reliably estimate the characterisation errors even in presence of model (shape) errors.

3.2. Milk characterisation by fat globule distributions

The solution of the ILS problem for individual MFGs allows us to construct the distributions over MFG characteristics of the milk samples. The distributions constructed from individual measurements can be characterised by statistical values such as mean value, standard deviation, median, mode (all based on number averaging). First, we compared the distribution parameters for the raw milk characterised using two optical models and combined into final results, presented in Table 1. Most of the parameters are almost identical similar for all three characterisation methods. It means that shape deviations of a real MFG from its optical model result in quasi-random variations of the determined parameters, which average out for the large enough sample. For instance, the diameter errors are much smaller for the combined method (as expected) but this has almost no effect on diameter distribution. There is however, a small model-dependent bias in RI. We suggest that such behaviour can be caused by the second term in the residual function [Eq. (2)]. This term mainly relates to the size of a particle measured from the angle-resolved light scattering and is insensitive to the refractive index and weak asphericity of the particle (Semyanov et al., 2004).

We also characterised MFGs be their specific surface area, defined as the ratio of total surface area of MFGs to their total volume. In particular, this parameter determines the capacity of MFGs for carrying bio-active molecules on their surface, which is relevant both for health aspects of milk and for manufacturing of dairy products. For spherical optical model specific surface area is completely determined by the size distribution, but the latter should be determined accurately in the whole size range.

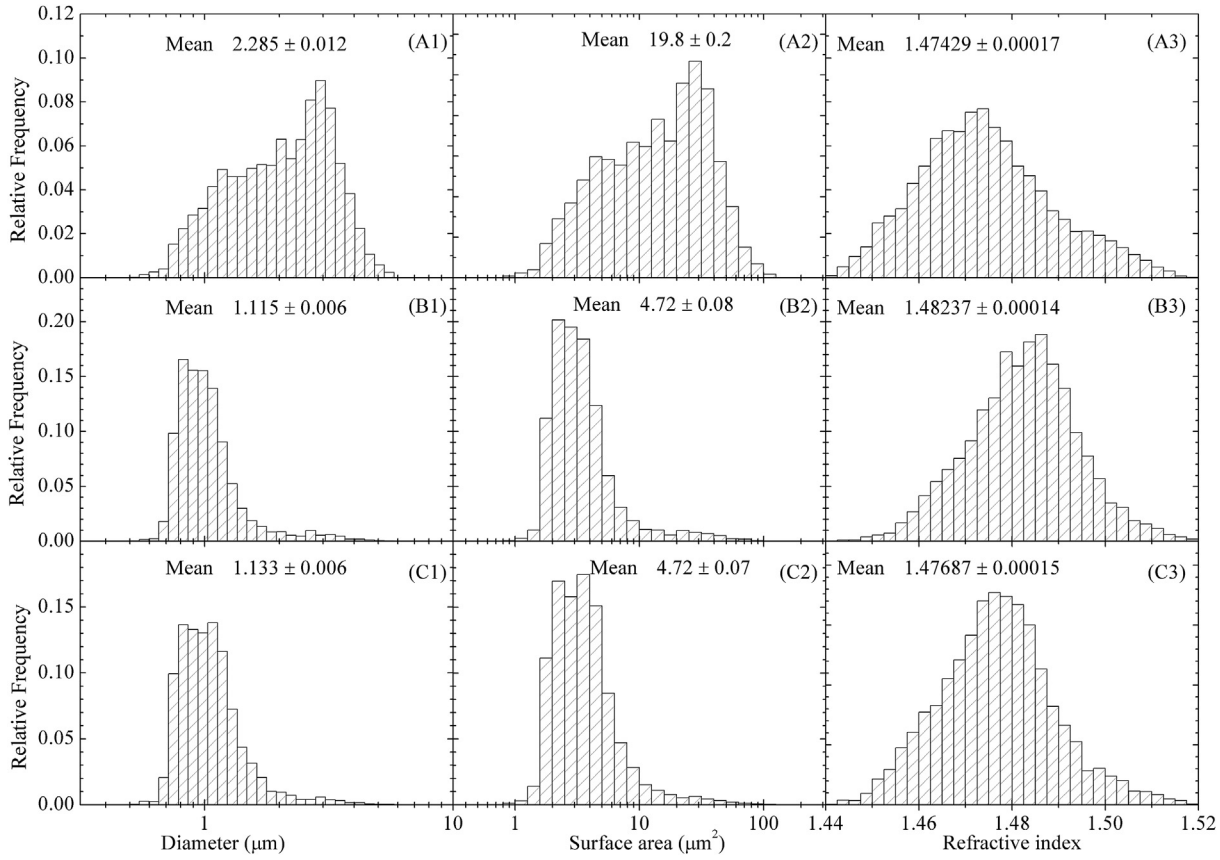

Fig. 5. The distributions over diameter, surface area, and refractive index of raw milk (A), and two samples of processed milk with 2.5% (B) and 3.2% (C) fat content.

This makes our definition different from (and more rigorous than) the commonly used one, computed from a mode of the size distribution obtained from low-angle light-scattering (Berton et al., 2012; Zamora et al., 2012). Moreover, spheroidal shape introduces dependence on ε, slightly increasing the specific surface area in comparison with the spherical model (Table 1).

We constructed the distributions over diameter, surface area and RI for three milk samples described in Section 2.1 (raw, 2.5%, and 3.2%). The normalised distributions for these samples are shown in Fig. 5, and distribution parameters – in Table 2. The distributions over MFG size are similar to the distributions published in numerous articles (Cheong et al., 2009; Fauquant et al., 2005; Garcia et al., 2014; Ong et al., 2010). The precision of single-particle size measurement is on average much better for the processed milk samples due to smaller sizes. The distributions over MFG surface area were calculated taking into account the optical model for the each MFG determined from the solution of the ILS problem. We did not see an analogous result elsewhere in research papers.

Table 2
Parameters of milk fat globules distributions of milk samples.

Parameter	Raw milk	Processed milk	
		2.5% Fat	3.2% Fat
Diameter (μm)			
Mean ± standard error of mean	2.285 ± 0.012	1.115 ± 0.006	1.133 ± 0.006
Standard deviation	1.022	0.504	0.465
Median	2.175	0.989	1.030
Refractive index			
Mean ± standard error of mean	1.47429 ± 0.00017	1.48237 ± 0.00014	1.47687 ± 0.00015
Standard deviation	0.0143	0.0117	0.0123
Surface area (μm^2)			
Mean ± standard error of mean	19.8 ± 0.2	4.72 ± 0.08	4.72 ± 0.07
Standard deviation	16.9	6.80	6.20
Median	14.9	3.08	3.33
Specific surface area (μm^{-1})	1.93	3.33	3.52
Well-described by spheres (%)	71	87	92
Error of diameter (nm)			
Mean	119	44	52
Median	74	23	30

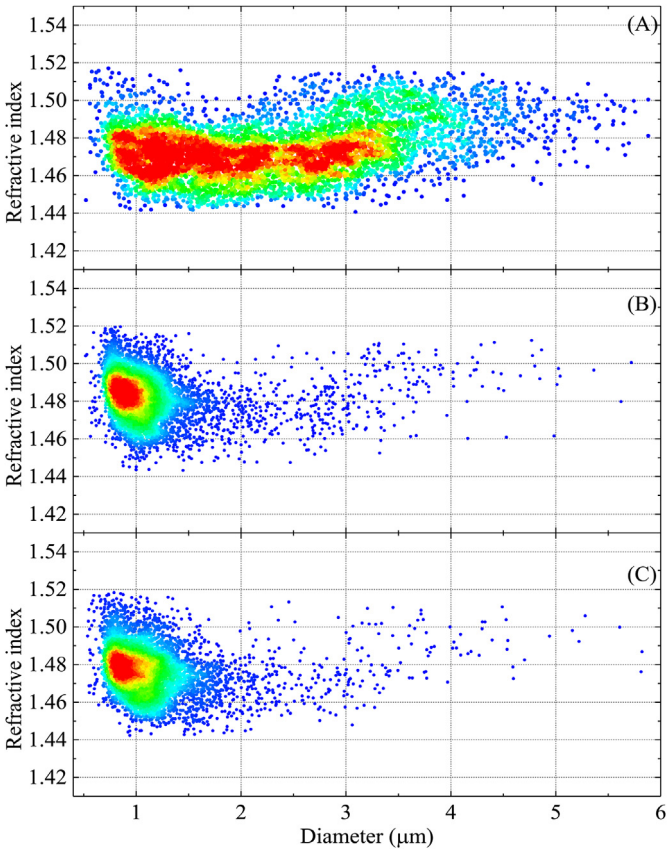

Fig. 6. Refractive index versus diameter coloured-density map of raw milk (A), and two samples of processed milk with 2.5% (B) and 3.2% (C) fat content.

The mean values of RI of MFGs (at $\lambda = 405$ nm) are reasonable in comparison with literature data: the index-matching method gave 1.470 and 1.460 for RI of MFGs at 466 nm and 633 nm respectively (Michalski et al., 2001), and single-particle measurement resulted in average RI of 1.464 at 633 nm (Cheong et al., 2009). The standard deviation of RI is 2–3 times smaller than that in Cheong et al. (2009), which indicates superior accuracy of our approach. Moreover, this standard deviation is comparable to single-particle characterisation errors, which suggests that natural intra-sample variation of MFG RI may be even smaller. The raw and processed milk samples are easily distinguishable from almost any of the distribution parameters, mostly from the diameter distribution. The two samples of processed milks can be distinguished from the MFG specific bio-capacities, and medians or standard deviations of surface area distributions.

Finally, we present an RI versus diameter scatterplot with a coloured density all analysed samples in Fig. 6. Similar to the case with distribution parameters, we can easy distinguish the native milk from commercial one and observe the weak difference between two samples of milk from manufacturers. Note also that the variability of RI does not noticeably increase with decreasing diameter, in contrast to artefacts present in Cheong et al. (2009) and our previous study on blood microparticles (Konokhova et al., 2012).

4. Conclusion

We have demonstrated an advanced performance of the scanning flow cytometry in characterisation of individual particles from light scattering. For the first time the shape of MFGs was modelled by an oblate spheroid to agree with sensitive measurement of angle-resolved light scattering. The LSP contains sufficient information about MFG morphology to provide the nanometer precision in determination of the individual MFG size from solution of the ILS problem. Additionally each MFG was characterised by its RI and surface area taking into account the asphericity of individual MFGs. We also characterised each milk sample by the specific surface area that can be calculated with good precision only with the developed method. This value can be taken into account during, for instance, normalisation of commercially manufactured milk. A number of statistical parameters of MFG distributions can be retrieved from the analysis for precise quantitative characterisation of milk samples. In the coming experiments we are going to clarify the role of MFG aggregates in formation of the MFG distributions similar to our study of light scattering from aggregates of polymer beads (Strokotov et al., 2011). We assume that an account of MFG aggregates will change the specific surface area of milk considerably because of its complex shape.

Based on its precision the scanning flow cytometer specially adapted for analysis of MFGs can become the base of a “gold standard” method to analyse MFGs. At present this method satisfies all requirements of dairy technologists who are developing new high-quality natural bioactive nutrition. Manufacturers will be able to fine control the conditions of technological equipment, e.g., homogeniser, to prevent quality loss during milk processing.

Acknowledgements

This work was supported by Russian Science Foundation (14-15-00155). D. I. Strokotov, A. E. Moskalensky and M. A. Yurkin also acknowledge the support by the Stipend of the President of Russian Federation for young scientists.

References

Argov, N., Lemay, D. G., & German, J. B. (2008). Milk fat globule structure and function: nanoscience comes to milk production. *Trends in Food Science and Technology, 19*, 617–623.
Beresford, T. P., Fitzsimons, N. A., Brennan, N. L., & Cogan, T. M. (2001). Recent advances in cheese microbiology. *International Dairy Journal, 11*, 259–274.
Berner, L. A. (1993). Defining the role of milk fat in balanced diets. In John E. Kinsella (Ed.), *Advances in food and nutrition research* (Vol. 37, pp. 131–257). San Diego, CA, USA: Academic Press.
Berton, A., Rouvellac, S., Robert, B., Rousseau, F., Lopez, C., & Crenon, I. (2012). Effect of the size and interface composition of milk fat globules on their in vitro digestion by the human pancreatic lipase: native versus homogenized milk fat globules. *Food Hydrocolloids, 29*, 123–134.
Bohren, C. F., & Huffman, D. R. (1983). *Absorption and scattering of light by small particles*. New York, NY, USA: Wiley.
Cheong, F. C., Xiao, K., & Grier, D. G. (2009). Technical note: characterizing individual milk fat globules with holographic video microscopy. *Journal of Dairy Science, 92*, 95–99.
Dewettinck, K., Rombaut, R., Thienpont, N., Le, T. T., Messens, K., & Van Camp, J. (2008). Nutritional and technological aspects of milk fat globule membrane material. *International Dairy Journal, 18*, 436–457.
El-Zeini, H. (2006). Microstructure, rheological and geometrical properties of fat globules of milk from different animal species. *Polish Journal of Nutrition Sciences, 56*, 147–154.
Fauquant, C., Briard, V., Leconte, N., & Michalski, M.-C. (2005). Differently sized native milk fat globules separated by microfiltration: fatty acid composition of the milk fat globule membrane and triglyceride core. *European Journal of Lipid Science and Technology, 107*, 80–86.
Freudenstein, C., Keenan, T. W., Eigel, W. N., Sasaki, M., Stadler, J., & Franke, W. W. (1979). Preparation and characterization of the inner coat material associated with fat globule membranes from bovine and human milk. *Experimental Cell Research, 118*, 277–294.
Fucà, N., Pasta, C., Impoco, G., Caccamo, M., & Licitra, G. (2013). Microstructural properties of milk fat globules. *International Dairy Journal, 31*, 44–50.
Gallier, S., Gragson, D., JimeNez-Flores, R., & Everett, D. (2010). Using confocal laser scanning microscopy to probe the milk fat globule membrane and associated proteins. *Journal of Agricultural and Food Chemistry, 58*, 4250–4257.
Garcia, C., Antona, C., Robert, B., Lopez, C., & Armand, M. (2014). The size and interfacial composition of milk fat globules are key factors controlling

triglycerides bioavailability in simulated human gastro-duodenal digestion. *Food Hydrocolloids, 35*, 494–504.
Heid, H. W., & Keenan, T. W. (2005). Intracellular origin and secretion of milk fat globules. *European Journal of Cell Biology, 84*, 245–258.
Hillbrick, G., McMahon, D., & Deeth, H. (1998). Electrical impedance particle size method (coulter counter) detects the large fat globules in poorly homogenized UHT processed milk. *Australian Journal of Dairy Technology, 53*, 17–21.
Huppertz, T., & Kelly, A. L. (2006). Physical chemistry of milk fat globules. In P. F. Fox, & P. L. H. McSweeney (Eds.), *Lipids: Vol. 2. Advanced dairy chemistry* (pp. 173–212). New York, NY, USA: Springer US.
Jones, D. R., Perttunen, C. D., & Stuckman, B. E. (1993). Lipschitzian optimization without the Lipschitz constant. *Journal of Optimization Theory and Applications, 79*, 157–181.
Konokhova, A. I., Gelash, A. A., Yurkin, M. A., Chernyshev, A. V., & Maltsev, V. P. (2013). High-precision characterization of individual *E. coli* cell morphology by scanning flow cytometry. *Cytometry Part A, 83A*, 568–575.
Konokhova, A. I., Yurkin, M. A., Moskalensky, A. E., Chernyshev, A. V., Tsvetovskaya, G. A., Chikova, E. D., et al. (2012). Light-scattering flow cytometry for identification and characterization of blood microparticles. *Journal of Biomedical Optics, 17*, 057006–057011.
Lauber, K., Keppeler, H., Munoz, L. E., Koppe, U., Schröder, K., Yamaguchi, H., et al. (2013). Milk fat globule-EGF factor 8 mediates the enhancement of apoptotic cell clearance by glucocorticoids. *Cell Death and Differentiation, 20*, 1230–1240.
Lopez, C. (2011). Milk fat globules enveloped by their biological membrane: unique colloidal assemblies with a specific composition and structure. *Current Opinion in Colloid and Interface Science, 16*, 391–404.
Maltsev, V. P. (2000). Scanning flow cytometry for individual particle analysis. *Review of Scientific Instruments, 71*, 243–255.
Maltsev, V. P., Chernyshev, A. V., Semyanov, K. A., & Soini, E. (1997). Absolute real-time determination of size and refractive index of individual microspheres. *Measurement Science and Technology, 8*, 1023–1027.
Maltsev, V. P., Chernyshev, A. V., & Strokotov, D. I. (2013). Light-scattering flow cytometry: advanced characterization of individual particle morphology. In S. Papandreou (Ed.), *Flow cytometry: Principles, methodology and applications* (pp. 79–103). New York, NY, USA: Nova Science Publishers.
Michalski, M.-C., Briard, V., & Michel, F. (2001). Optical parameters of milk fat globules for laser light scattering measurements. *Lait, 81*, 787–796.
Miles, C. A., Shore, D., & Langley, K. R. (1990). Attenuation of ultrasound in milks and creams. *Ultrasonics, 28*, 394–400.
Mishchenko, M. I., & Travis, L. D. (1998). Capabilities and limitations of a current FORTRAN implementation of the T-matrix method for randomly oriented, rotationally symmetric scatterers. *Journal of Quantitative Spectroscopy and Radiative Transfer, 60*, 309–324.
Mishchenko, M. I., Travis, L. D., & Mackowski, D. W. (2014). *NASA GISS: Scattering—T-matrix codes*. Available at http://www.giss.nasa.gov/staff/mmishchenko/t_matrix.html Accessed 21.04.14.
Moskalensky, A. E., Yurkin, M. A., Konokhova, A. I., Strokotov, D. I., Nekrasov, V. M., Chernyshev, A. V., et al. (2013). Accurate measurement of volume and shape of resting and activated blood platelets from light scattering. *Journal of Biomedical Optics, 18*, 017001–017012.
Ong, L., Dagastine, R. R., Kentish, S. E., & Gras, S. L. (2010). The effect of milk processing on the microstructure of the milk fat globule and rennet induced gel observed using confocal laser scanning microscopy. *Journal of Food Science, 75*, E135–E145.
Robin, O., & Paquin, P. (1991). Evaluation of the particle size of fat globules in a milk model emulsion by photon correlation spectroscopy. *Journal of Dairy Science, 74*, 2440–2447.
Semyanov, K. A., Tarasov, P. A., Soini, J. T., Petrov, A. K., & Maltsev, V. P. (2000). Calibration-free method to determine the size and hemoglobin concentration of individual red blood cells from light scattering. *Applied Optics, 39*, 5884–5889.
Semyanov, K. A., Tarasov, P. A., Zharinov, A. E., Chernyshev, A. V., Hoekstra, A. G., & Maltsev, V. P. (2004). Single-particle sizing from light scattering by spectral decomposition. *Applied Optics, 43*, 5110–5115.
Singh, H. (2006). The milk fat globule membrane—A biophysical system for food applications. *Current Opinion in Colloid and Interface Science, 11*, 154–163.
Soini, J. T., Chernyshev, A. V., Hänninen, P. E., Soini, E., & Maltsev, V. P. (1998). A new design of the flow cuvette and optical set-up for the scanning flow cytometer. *Cytometry, 31*, 78–84.
Spitsberg, V. L. (2005). Invited review: bovine milk fat globule membrane as a potential nutraceutical. *Journal of Dairy Science, 88*, 2289–2294.
Strokotov, D. I., Moskalensky, A. E., Nekrasov, V. M., & Maltsev, V. P. (2011). Polarized light-scattering profile—advanced characterization of nonspherical particles with scanning flow cytometry. *Cytometry Part A, 79A*, 570–579.
Strokotov, D. I., Yurkin, M. A., Gilev, K. V., van Bockstaele, D. R., Hoekstra, A. G., Rubtsov, N. B., et al. (2009). Is there a difference between T- and B-lymphocyte morphology? *Journal of Biomedical Optics, 14*, 064036.
Su, J., & Everett, D. W. (2003). Adsorption of κ-casein onto native milk fat globule, latex particle, and emulsion surfaces. *Food Hydrocolloids, 17*, 529–537.
Thiebaud, M., Dumay, E., Picart, L., Guiraud, J. P., & Cheftel, J. C. (2003). High-pressure homogenisation of raw bovine milk. Effects on fat globule size distribution and microbial inactivation. *International Dairy Journal, 13*, 427–439.
Van Kreveld, A. (1942). The size distribution of fat globules in milk. *Recueil Des Travaux Chimiques Des Pays-Bas, 61*, 29–40.
Wriedt, T. (2008). Mie theory 1908, on the mobile phone 2008. *Journal of Quantitative Spectroscopy and Radiative Transfer, 109*, 1543–1548.
Yurkin, M. A., Semyanov, K. A., Tarasov, P. A., Chernyshev, A. V., Hoekstra, A. G., & Maltsev, V. P. (2005). Experimental and theoretical study of light scattering by individual mature red blood cells by use of scanning flow cytometry and a discrete dipole approximation. *Applied Optics, 44*, 5249–5256.
Zamora, A., Ferragut, V., Guamis, B., & Trujillo, A. J. (2012). Changes in the surface protein of the fat globules during ultra-high pressure homogenisation and conventional treatments of milk. *Food Hydrocolloids, 29*, 135–143.